

JULITA JAKUBIAK^{*)}, JAN F. RABEK^{**)}

Three-dimensional (3D) photopolymerization in stereolithography^{***)}

PART I. FUNDAMENTALS OF 3D PHOTOPOLYMERIZATION

"Stereolithography is like black art. You can build a part any number of ways, but the more you experience the process, the better you'll do"

William J. Coleman

Summary — A review with 77 refs. covering the fundamentals of three-dimensional photopolymerization (3DP), *viz.*, resin formulations (photoinitiators and monomers) for stereolithography, layer-by-layer space-resolved 3DP process, multiphotonic 3DP, optimization of 3DP parameters, volume contraction (shrinkage) and curl distortion in 3DP and applications of 3DP stereolithographic models.

Key words: three-dimensional photopolymerization, photoinitiators for 3D polymerization, layer-by-layer space-resolved 3 D photopolymerization, resin formulation for stereolithography.

Three-dimensional (3D) photopolymerization (stereolithography) is a new technology [1—18] linking the computer models (Computer Aided Design (CAD) [13, 17—19]) and Computer Aided Manufacturing (CAM) processes [13, 17—23] to the Rapid Prototyping and Manufacturing (RPM) of a polymer solid, shaped product [13, 17—19]. In this method a laser beam, driven by a 3D-CAD-CAM system across an x,y -surface, is used to form point by point, layer by layer a solid polymer object by photopolymerizing an acrylate resin. Within the last decade, several fully automated industrial 3D-CAD-CAM Solid Creation Systems (SCS) have been made available [13, 16—19, 24].

In Europe, two research centers, *viz.*, Ciba-Geigy Ltd. Marly Works Research Center, CH-1701 Fribourg, Switzerland [15], and GRAPP-URA 328 CNRS, ENSIC-INPL, BP 451, 1 rue Grandville, F-54001 Nancy Cedex, France [17], are the centers most advanced in stereolithography. Professor J. P. Fouassier (Laboratoire de Photochimie Generale CNRS No. 431, ENSCMU, 3 rue Alfred Werner, F-68200, Mulhouse Cedex, France) has been guiding the fundamental research on laser photoinitiation, photopolymerization, and photocuring, which are the basic techniques to evaluate resins to be used for stereolithographic purposes [25]. Professor J. Pączkowski (De-

partment of Physical Chemistry, University of Technology and Agriculture, Bydgoszcz, Poland) has developed a 3D photopolymerization program in Poland. Dr. J. Jakubiak of the Department of Chemistry, Jagiellonian University, Cracow, heads an international project on photopolymerization in cooperation with Prof. J. F. Rabek (Sweden).

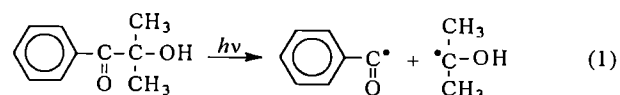
RESIN FORMULATIONS FOR STEREOLITHOGRAPHY

3D photopolymerization requires a rapid photochemical process [17, 25—27], and many photoinitiators and monomers fail on these counts. The composition of the resin formulation is the key factor in the 3D photopolymerization process since it directly determines the final product and the mechanical properties of the model. Current UV-sensitive formulations include a carefully selected UV-photoinitiator, a co-initiator, different monomers and oligomers, and additives.

Photoinitiators for 3D polymerization

Three types of UV photoinitiators commonly used for initiation of 3D polymerization include:

— photoinitiators which undergo an intramolecular photocleavage into two radicals (Table 1) [15, 17, 26—32]:



— photoinitiators which produce free radicals by intermolecular hydrogen abstraction from a hydrogen donor molecule (co-initiator) by the Electron/Proton Transfer (EPT) [26—32]; this type of photoinitiators is exemplified by benzophenones, diketones and thioxan-

^{*)} Department of Chemistry, Jagiellonian University, Ingardena 3, 30-060 Cracow, Poland. To whom all correspondence should be addressed.

^{**)} Polymer Research Group, Department of Dental Biomaterial Science, Karolinska Institute (Royal Academy of Medicine), Box 4064, 141 04 Huddinge (Stockholm), Sweden, and Department of Chemistry and Chemical Engineering Technical and Agricultural University, Seminaryjna 3, 85-326 Bydgoszcz, Poland.

^{***)} This paper was partially presented at the Chemical Forum organized by Prof. M. Jarosz at the Technological University, Warsaw, May 2000, and is dedicated by the Authors to Professor T. Sikorski of the Department of Organic and Polymer Technology, Technical University, Wrocław, Poland, on the occasion of his 70th birthday.

Table 1. Typical UV photoinitiators used in the 3D photopolymerization

Chemical name	Chemical structure	Commercial name and supplier	Absorption, nm
Substituted alkyl aryl ketones		Sandoray 100 (Sandoz)	240–360
Phenyl-2-hydroxy-2-propyl ketone		Darocure 1173 (Ciba-Geigy)	250–350
2,2-Dimethoxy-2-phenyl acetophenone (benzyl-dimethyl ketal) (2,2-dimethoxy-1,2-diphenyl-ethan-1-one)		Irgacure 651 (Ciba-Geigy)	250–350
2-Methyl-1-(4-methylthiophenyl)-2-morpholino propan-1-one		Irgacure 907 (Ciba-Geigy)	230–360
1-Hydroxy-cyclohexyl-phenyl ketone		Irgacure 184 (Ciba-Geigy)	331
1-Phenyl-1,2-propanedione-2-o-ethoxycarbonyl oxime		Quantacure PDO (AcetoChemical)	275–400
Bis(2,6-dimethoxybenzoyl)-2,4,4-trimethylpentyl-phosphine oxide		BAPO (Ciba-Geigy)	380

thones (Table 2); the most common hydrogen-atom donors are amines:

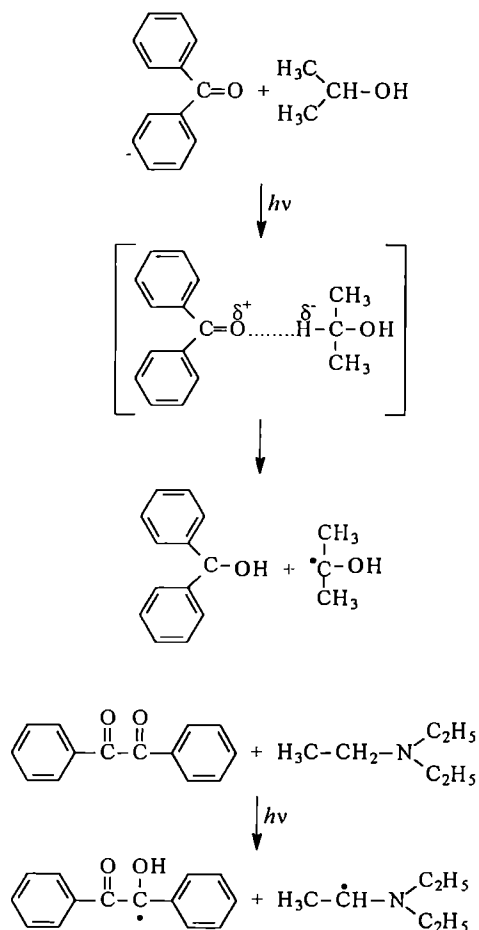


Table 2. Photoinitiators which produce free radicals by intermolecular hydrogen abstraction from a hydrogen donor molecule (coinitiator)

Chemical name	Structure	Absorption, nm
Benzophenone		220–300
Camphorquinone		480
Thioxanthone		260

— cationic photoinitiators (Table 3) [15, 25, 26, 33–36].

The primary step in the photolysis of the diaryliodonium cation is the homolytic bond cleavage to yield the aryliodonium radical cation, $ArI^{\bullet+}$, and an aryl radical ($Ar\bullet$). The H-atom abstraction from the monomer (MH) is postulated to result in the radical $M\bullet$ and in the protonated aryl iodide which dissociates into H^+X^- and ArI [33–36]:

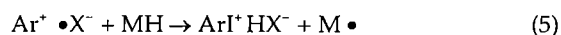
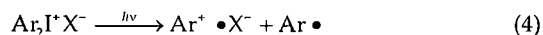
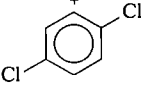
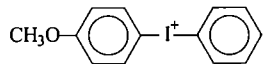
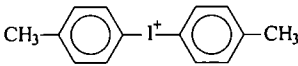
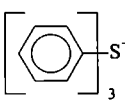
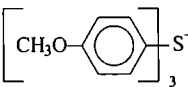
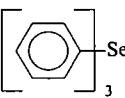
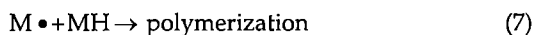
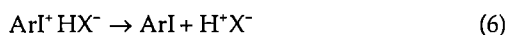


Table 3. Cationic photoinitiators

Cation	Anion	Absolute maxima, nm
	SbF ₆ ⁻	238, 358
	BF ₄ ⁻	246
	PF ₆ ⁻	237
	BF ₄ ⁻	230
	AsF ₆ ⁻	225, 280
	BF ₄ ⁻	258, 266, 275



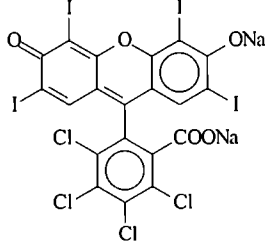
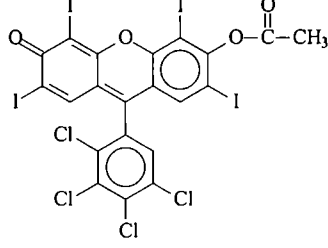
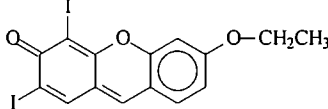
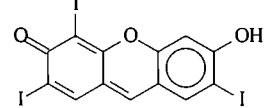
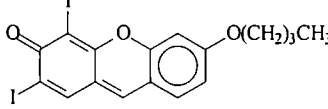
In these onium salts, typical non-nucleophilic anions are BF₄⁻, ClO₄⁻, CF₃SO₃⁻, PF₆⁻, AsF₆⁻ and SbF₆⁻. Anions Cl⁻, Br⁻, or I⁻, bases, water and hydroxyl-containing compounds quench the cation formation and inhibit polymerization. Unlike radical polymerizations, oxygen does not inhibit cationic polymerization. Dyes like acridine orange and benzoflavin efficiently sensitize cationic polymerization in the visible light range [37].

Visible light 3D photopolymerization is mainly based on:

— fluorinated diaryltitanocene [38] and a chloromethyl substituted triazine [39] (Table 4);

— dye photoinitiators, e.g. xanthenes, modified xanthenes, fluorones (Table 5) in the presence of different

Table 5. Examples dye visible light photoinitiators used in the 3D photopolymerization [47]

Chemical structure	Chemical name	Absorption λ _{max} , nm
Xanthene dyes:		
	Rose Bengal	548
	RBAX	492
Fluorone dyes:		
	DIEF	470
	TIHF	538
	DIBF	470

co-initiators (Table 6) [28, 40—46]. Most visible photoinitiators function by the EPT mechanism in which the light absorbing dye is either oxidized or reduced in the

Table 4. Typical visible light photoinitiators used in the 3D photopolymerization

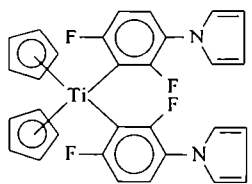
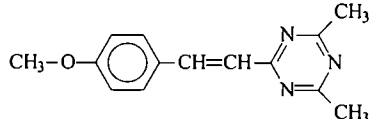
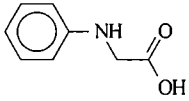
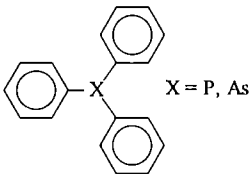
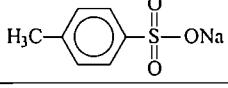
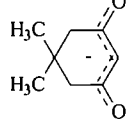
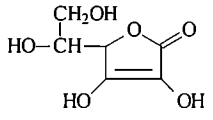
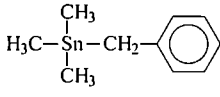
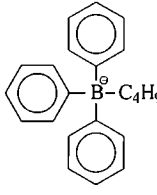
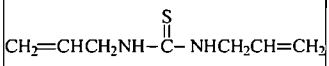
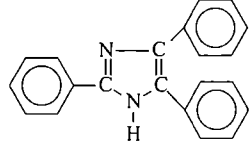
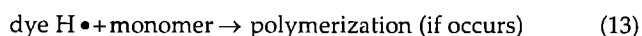
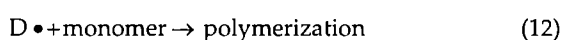
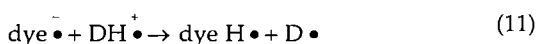
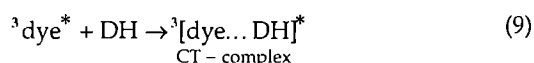
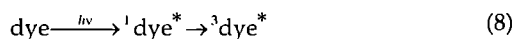
Chemical name	Chemical structure	Commercial name and supplier	Absorption, nm
Fluorinated diaryltitanocene		Irgacure 784 (Ciba-Geigy)	450—500
Methyl substituted triazine		(Hoechst)	488

Table 6. Coinitiators for photoreducible dyes [28]

Type	Chemical structure	Chemical name
Amines	$N(C_2H_5OH)_3$	Triethanolamine
Aminoacids		<i>N</i> -Phenylglycine
Phosphines/Arsines	 X = P, As	Triphenylphosphine Triphenylarsine
Sulphinates		Sodium <i>p</i> -tolylsulphinate
Enolates		Dimedone enolate
Carboxylates and/or lactones		Ascorbic acid
Organotin compounds		Benzyltrimethylstannane
Borates		Triphenylbutylborate
Miscellaneous		Diallylthiourea
		2,4,5-Triphenylimidazole

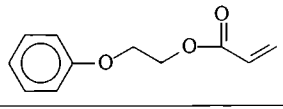
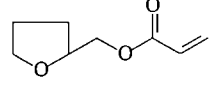
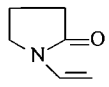
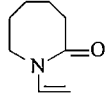
excited singlet or triplet state and EPT occurs in the presence of a hydrogen atom donor co-initiators according to the mechanisms [47]:



Monomers and formulated resins

Resins for 3D photopolymerization consist of combinations of mono- (Table 7), di- (Table 8), multi- (Table 9), oligomeric and polymeric multifunctional (Table 10) monomers [15, 17]. Recently epoxy, epoxyacrylates and urethane acrylates have also been used [27, 48]. A typical formulation for the He-Cd laser induced 3D photopolymerization is shown in Table 11.

Table 7. Monofunctional monomers [15]

Chemical name	Chemical structure
2-Phenoxyethyl acrylate	
Tetrahydrofurfuryl acrylate	
<i>N</i> -Vinylpyrrolidone	
<i>N</i> -Vinylcaprolactam	

Multifunctional acrylate resin formulations are generally 1,000 centipoise or more in viscosity at room temperature (25–30°C). At these viscosities, the resins behave as thick syrups that flow very slowly. For 3D photopolymerization, moderately high viscosity (>1,000 cP) results in lower throughput, longer recoating times, and more difficult removal of unwanted air bubbles from the resin. To lower the viscosity of the resins, monofunctional monomers (most commonly *N*-vinylpyrrolidone (Table 8)) are added. After laser irradiation, the resin forms an insoluble, highly crosslinked gel. The newly formed part is characterized as being "green", in the sense that it still has unchanged monomers that can be cured in a post-irradiation or in post-thermal steps. The strength of the green part is related to the cross-link density of the part. It must be sufficiently high to [49]:

— permit detailed product formation;

— minimize swelling;

— permit handling prior to the post curing processes.

The acrylate-based systems also require a high green strength (or high crosslink density) in the green part, to minimize post-cure distortion effect. A high crosslink density yields strong parts; the acrylates lack toughness, however. The lack of toughness can also give rise to part fracture when stress is relieved in large and complicated parts during a post-cure step. Since acrylate systems are highly crosslinked in the green state (to minimize post cure distortion), large or complex geometry parts exhibit variability in the degree of cure. In addition, the UV post cure irradiation is not isotropic, owing

Table 8. Difunctional monomers [15]

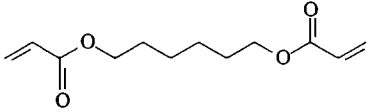
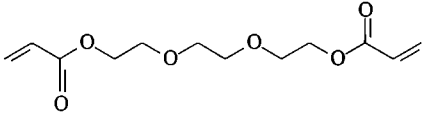
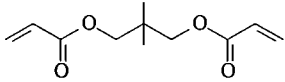
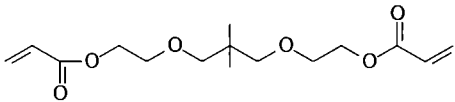
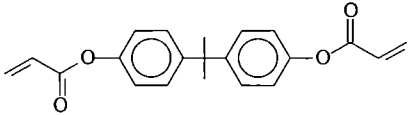
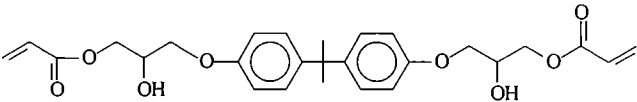
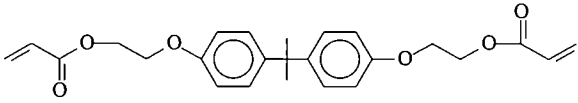
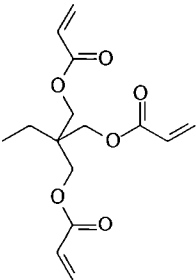
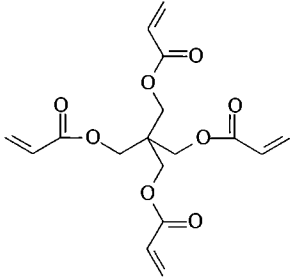
Chemical name	Chemical structure
Aliphatic diacrylates (linear)	
Hexanedioldiacrylate	
Triethyleneglycol diacrylate	
Aliphatic diacrylates (branched)	
Neopentylglycol diacrylate	
Ethoxylated neopentylglycol diacrylate	
Aromatic diacrylates	
Bisphenol-A-diacrylate	
Bisphenol-A-diepoxydiacrylate	
Ethoxylated bisphenol-A-diacrylate	

Table 9. Multifunctional monomers [15]

Chemical name	Chemical structure
Trimethylolpropane triacrylate	
Pentaerythritol tetraacrylate	

to a non-uniform light flux, resulting from variable thickness throughout the part. Acrylate resins are brittle due to the nature of their chemical structure. Formulations are limited in improving the mechanical properties without sacrificing viscosity, cure speed and strength.

For photocationic polymerization mainly epoxides (Table 12), vinyl ethers and urethane vinyl ethers have been used [15]. These monomers allow the mechanical end properties of 3D models to be finely designed.

It goes beyond the scope of this review to describe in any details all the resin formulations available for photopolymerization; this subject has been amply reviewed [15, 27, 40, 50] and approached in monographs [25, 26, 29]. The kinetic modelling of linear and crosslinking photopolymerization has been discussed in detail [51, 52]. The computerized kinetic model of the 3D laser photopolymerization, which takes the viscosity phenomena and gel point into special account, has been described elsewhere [53].

Table 10. Oligomeric and polymeric multifunctional monomers [15]

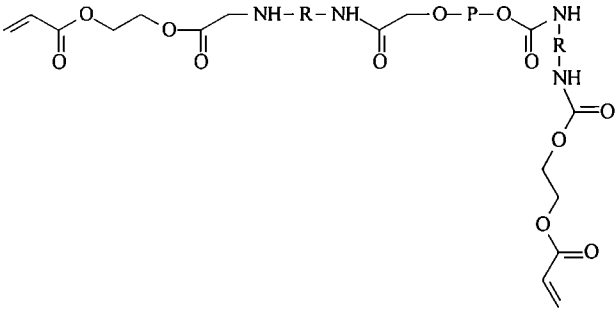
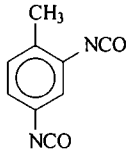
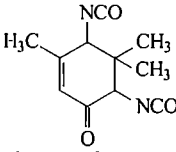
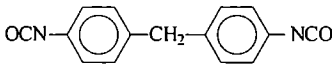
Chemical name	Chemical structure
Urethane acrylates	 <p data-bbox="678 541 1310 569">P: Polyether, polyester; R: aromatic or aliphatic diisocyanates, e.g.:</p> <div style="display: flex; flex-direction: column; align-items: center;"> <div data-bbox="926 590 1052 741">  <p data-bbox="852 750 1130 778">Toluylene diisocyanate (TDI)</p> </div> <div data-bbox="903 789 1078 940">  <p data-bbox="874 935 1107 963">Isophorone diisocyanate</p> </div> <div data-bbox="824 978 1157 1043">  <p data-bbox="812 1047 1169 1075">Diphenylmethane diisocyanate (MDI)</p> </div> </div>

Table 11. Resin formulation for HeCd laser 3D photopolymerization [15]

Part by weight	Component
46	Bisphenol-A-diglycidyl-diacylate
23	Ethoxylated bisphenol-A-dimethacrylate
17	Dipentaerythritol pentaacrylate
5	2-Phenoxyethyl acrylate
5	N-Vinylpyrrolidone
4	1-Hydroxycyclohexyl-phenylketone

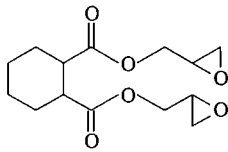
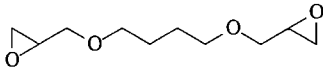
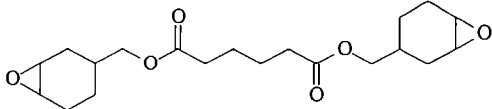
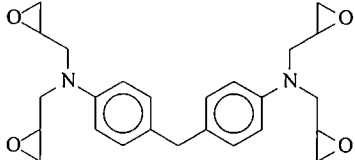
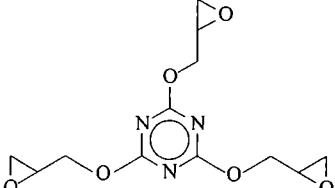
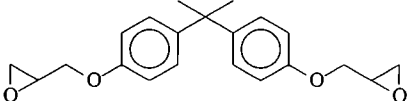
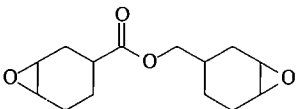
1	2
	CY 184
	DY 026
	CY 177
	MY 720
	PT 810

Table 12. Epoxy resins for photocationic polymerization [15]

Chemical formula	Trade names
1	2
	Araldite GY 250 GY 2600 MY 790
	CY 179

LAYER-BY-LAYER SPACE-RESOLVED 3D PHOTOPOLYMERIZATION

In this 3D photopolymerization, a portion of the open layer of a monomer is irradiated by a UV laser (excimer or YAG lasers), where upon a new layer of the monomer is added and polymerized and so on, until a complete object is manufactured (Fig. 1) [5, 17, 53, 54]. Poly-

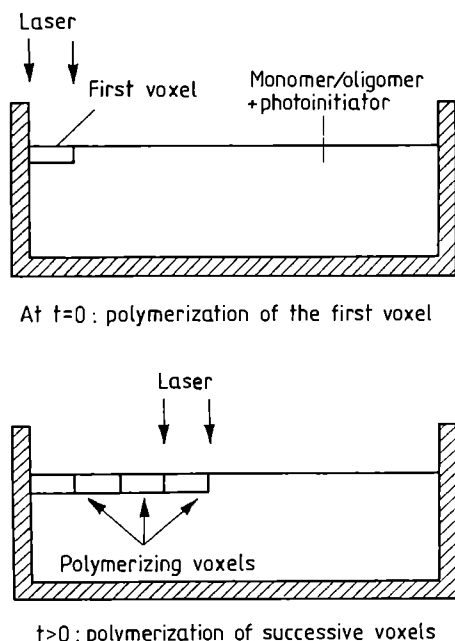


Fig. 1. Principle of layer-by-layer space-resolved 3D photopolymerization by a laser beam [5, 54]

merization occurs in a volume element called the *voxel*. Every laser pulse polymerizes a voxel. Successive polymerization occurs by polymerizing voxel after voxel.

Absorption of the laser radiation

The laser radiation passing through the resin composite layer should be completely absorbed by photoinitiators. However, only very small amounts of photons are absorbed in the micro-layer of the resin composite, and most of the exposure light passes straight through the material. The laser light is not absorbed homogeneously by the composite layer but, according to the exponential Beer-Lambert law, decreases exponentially with depth (x) [5, 15, 55]:

$$\frac{dI}{dx} = I_0 \exp(-x\epsilon_i[A]) \tag{14}$$

or

$$\frac{dI}{dx} = I_0 \exp(-xD_p) \tag{15}$$

where

$$D_p = \epsilon_i[A] \tag{16}$$

where I_0 is the intensity of incident laser beam, ϵ_λ is the monophotonic absorption (molar extinction) coefficient of a photoinitiator at wavelength λ , $[A]$ is the concentration of absorbing species (photoinitiator), and D_p is the light penetration depth at the laser wavelength (λ). In practice, the polymerization does not proceed beyond a limited depth where laser intensity is below a threshold value.

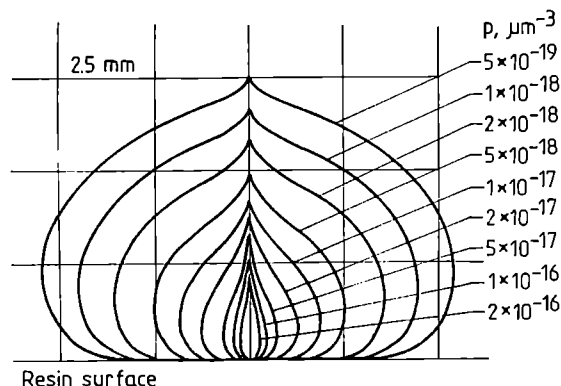


Fig. 2. The distribution of photon absorption [55]

Figure 2 shows the distribution of photon absorption, and indicates the cross-sectional progress in the polymerization of a solidified cell. Parameter p means the probability that a photon is absorbed in a unit volume per one photon input:

$$\frac{dI}{dx} = pI_0^2[A] \tag{17}$$

The absorption p of n identical photons by a molecule A is proportional to the n th power of the excitation laser flux (I) (photon \cdot cm $^{-2}$ \cdot s $^{-1}$) [15].

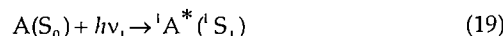
Multiphotonic 3D photopolymerization

Multiphotonic 3D photopolymerization is based on the absorption of two photons (differing in energies, $E_1 = h\nu_1$ and $E_2 = h\nu_2$) by a photoinitiating system [3, 5, 56—58]. The energies of the two photons must satisfy the following conditions:

$$h\nu_1 + h\nu_2 > E_d \tag{18}$$

with $h\nu_1 < E_d$ and $h\nu_2 < E_d$, where E_d is the energy of dissociation of a photoinitiator into free radicals.

The photoinitiator molecule (A) absorbs first photon E_1 and is excited to the singlet excited state 1S_1 and by inter system crossing (ISC) to the triplet excited state 3T_1 (Fig. 3):



One of this "intermediate" states, $^1A^*(^1S_1)$ or $^3A^*(^3T_1)$, absorbs the second photon E_2 (singlet-singlet absorption or triplet-triplet absorption) and is excited to higher n -states, 1S_n or 3T_n , whose excitation energy is higher

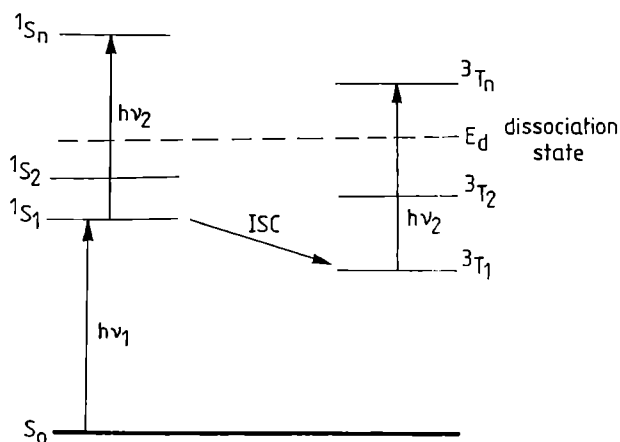
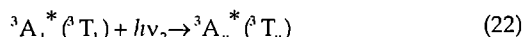
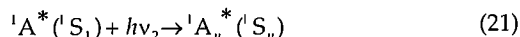


Fig. 3. Energy diagram of a biphotonic reaction: S_0 is the initial ground state of a photoinitiator molecule, 1S_1 or 3T_1 are the singlet or triplet "intermediate" excited states formed after absorption of a photon with energy $E_1 = hv_1$; 1S_n or 3T_n are higher singlet and triplet excited states formed after absorption of a second photon with energy $E_2 = hv_2$ and E_d is the energy of the dissociation state of a photoinitiator into free radicals

than the energy of dissociation of a photoinitiator into free radicals (E_d):



The "intermediate" states $^1A^*(^1S_1)$ or $^3A^*(^3T_1)$ must be in long-lived photochemically unreactive excited states and have a high quantum efficiency. For that reason the triplet-triplet absorption is the most acceptable photochemical process.

In this two-beam process, originating from upper excited states, a few photoinitiators like ketones (benzophenone), diketones (benzil) and 9-halofluorenones, can be activated only after they absorb two photons of different but well-known wavelengths [58—63]. Polymerization will be initiated only in the volume in which two light beams of the proper wavelengths intersect.

The amount of the radiations of two lasers absorbed by a photoinitiating system is given by the modified Beer-Lambert equation:

$$\frac{dI}{dx} = \delta I_{0(v_1)} I_{0(v_2)} [A] \quad (23)$$

where δ is the biphotonic absorption coefficient $I_{0(v_1)}$ and $I_{0(v_2)}$ are intensities of two lasers beams 1 and 2, and $[A]$ is the concentration of absorbing species (photoinitiator).

The problem which can limit multiphotonic initiation of polymerization is the differences in the refractive indices of resin composite: monomers, oligomers and finally crosslinked polymer, which are not equal and uniform during the polymerization reactions. The refractive index can change locally due to temperature rise, as each photopolymerization is an exothermic reaction.

Optimization of the 3D polymerization parameters

The CAD models [17, 20—23] for a laser induced 3D photopolymerization process couple the irradiation parameters [16—18], chemical and polymerization reactions kinetics, and heat transfer equations. Quantities which should be predicted include: spatial variations in light intensity, absorbed light, conversion of monomer to polymer, depletion of photoinitiator, and local variations of temperature in and around the spot contacted by the laser (heat of polymerization). In addition, physical data such as: rate constants of photoinitiation, propagation and termination (temperature dependent) for polymerization, heat of polymerization, heat capacity, thermal conductivity, density of monomer/polymer are required. This allows predictions to be made about the laser dwell time, depth penetration, and uniformity of the photopolymer formed in the 3D process.

The relationship between the cure depth (thickness of the exposed layer) (C_d) for a single laser cured line and the applied laser maximum energy (E_{max}) is called the "working curve", and is given by the equation:

$$C_d = D_p \ln(E_{max} / E_c) \quad (24)$$

where D_p is the light "penetration depth", and E_c is the "critical exposure" at which solidification starts to occur [16, 64]. Equation (24) states, in the mathematical form, the following basic points [16, 65]:

- the cure depth is proportional to the natural logarithm of the maximum exposure on the centerline of the scanned laser beam;

- a semilog plot of C_d versus E_{max} should be a straight line;

- the slope $\Delta C_d / \Delta \ln E$ of the "working curve" is precisely D_p , the penetration depth of a resin, at a given laser wavelength;

- the intercept of the "working curve", specifically the value of the exposure at which the cure depth is zero, is simply E_c , the critical exposure of a resin, at a given laser wavelength;

- since D_p and E_c are resin parameters, then both the slope and the intercept of the "working curve" are independent of laser power.

A higher exposure will gradually increase the degree of cure, but the cure depth is given by the thickness of the layer. The accurate determination of the variables that define the "working curve" for the resin mixture is the most important factor in controlling the accuracy of the stereolithographic process.

The "maximum cured linewidth" (L_{max}) is defined as [16]:

$$L_{max} = B(C_d / 2D_p)^{1/2} \quad (25)$$

where B is the laser spot diameter. This "maximum cured linewidth" function shows that for a Gaussian laser scanned in a straight line across a photopolymerizing layer obeying the Beer-Lambert Law of absorption:

- the cured linewidth, (L_{max}), is directly proportional to the laser spot diameter (B);
- the cured linewidth is also proportional to the square root of the ratio of the cure depth to the resin penetration depth (C_d/D_p);
- thus, a deeper curing will result in an increased linewidth; for that reason, it is very important to determine "the line width compensation factor" (algorithm in software) for the photosensitive material used;
- the line width in the stereolithographic process is, in part, influenced by the amount of light scattering present in the resin mixture. Light scattering is the consequence of certain additives that can be added to photopolymer to achieve the desired balance of imaging and/or physical properties (e.g., fillers [66]).

Volume contraction (shrinkage) and curl distortion in the 3D photopolymerization

Polymerization cause linear and volume contractions (shrinkages). The shrinkage that occurs during polymerization arises from different causes:

- The major factor relates to the fact that monomers are located at Van der Waals distances from one another, while in the corresponding polymer the (mono)mer units have moved to within a covalent radius which is approximately 1/3 of the Van der Waals radius. This causes the shrinkage that is roughly related to the number of mono(mer) units per unit volume converted to polymer.

- The change in entropy and the relative free volumes of monomer and polymer. Free volume is primarily determined by the packing efficiency of the macromolecules. Crystalline (and to some extent semi-crystalline) polymers are, for example, more closely packed than the corresponding amorphous polymers.

The shrinkage depends on various parameters such as: laser flux intensity, irradiation time, curing depth

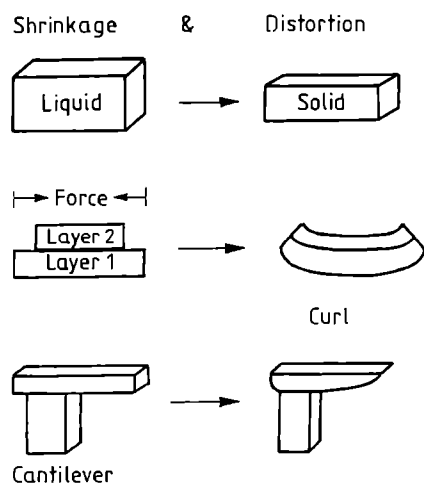


Fig. 4. Physical representation of geometric distortion resulting from anisotropic shrinkage [70]

and resin composition (type of photoinitiator, monomers and their ratio) [5, 15, 53, 54].

The linear and volume shrinkage (3—15%) [67], causes distortion such as curl (Fig. 4) [68, 69] and internal stress in final products. The solidification process occurs after the passage of the laser beam (Fig. 5). The shrinkage continues after the layer has become attached to the layer below. This shrinkage generates the stress perpendicular to the beam path, which cause the attached layer to curl.

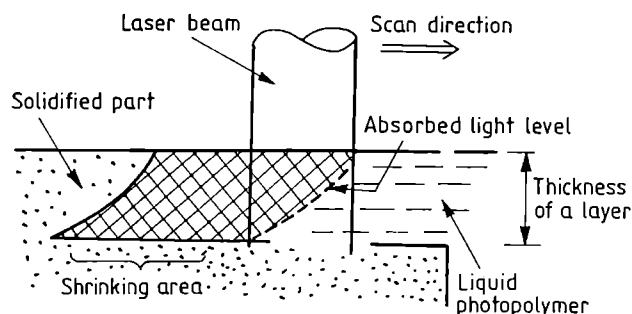


Fig. 5. Schematic side view of moving laser beam incident on resin (postirradiation shrinkage area is shown crosshatched) [69]

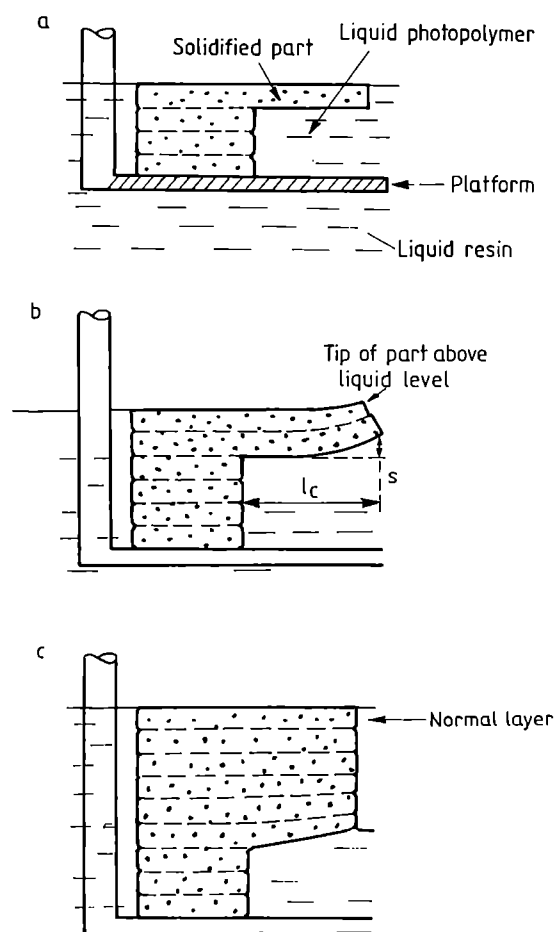


Fig. 6. Schematic side view of part building leading the curl: (a) first layer of cantilever, (b) second layer of cantilever and (c) after many layers [69]

Curl distortion, is a phenomenon characterized by bending of multiple unsupported cantilevered parts where the solidifying resin undergoes shrinkage (Fig. 6) [5, 53, 54, 69, 70]. Curl distortion can be manifested in a variety of forms (Fig. 7). It is desirable to minimize curl distortion, because higher part accuracy can then be achieved. A high curl distortion requires ancillary support structures of the photofabricated parts.

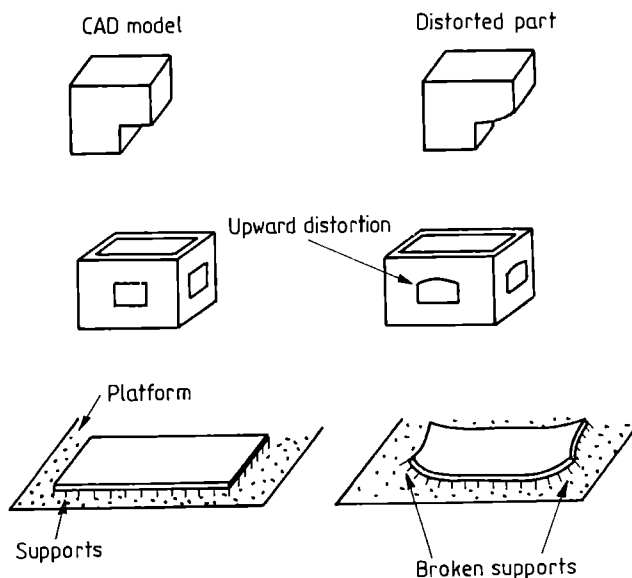


Fig. 7. Comparison of CAD models with distorted parts by the curl [69]

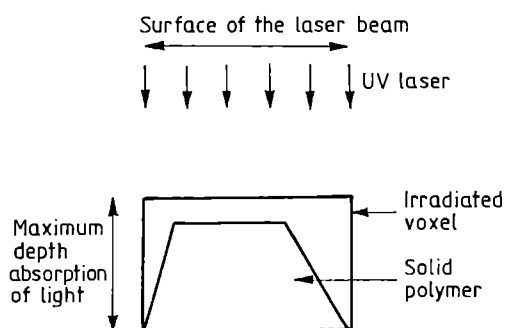


Fig. 8. The shrinkage of a voxel vs. irradiation depth [53]

The total deformation in the layer-by-layer space-resolved 3D photopolymerization depends on the deformation of every polymerized volume element (voxel) (Fig. 8) and on the way these elementary deformations combine with themselves (memory effect) to give a warping effect (Fig. 9) [5, 53]. A simulation model of geometrical deformations, based on the hypothesis of homogeneous shrinkage and viscoelastic properties of the polymerizing medium, has been developed [53]. Figure 10 shows the computer simulations of polymer shrinkage.

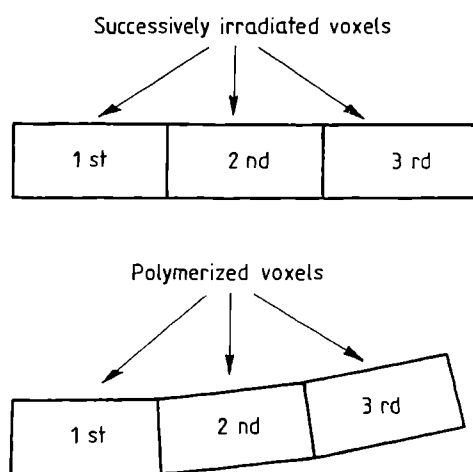


Fig. 9. Warping of a polymerized bar resulting from shrinkage [53]

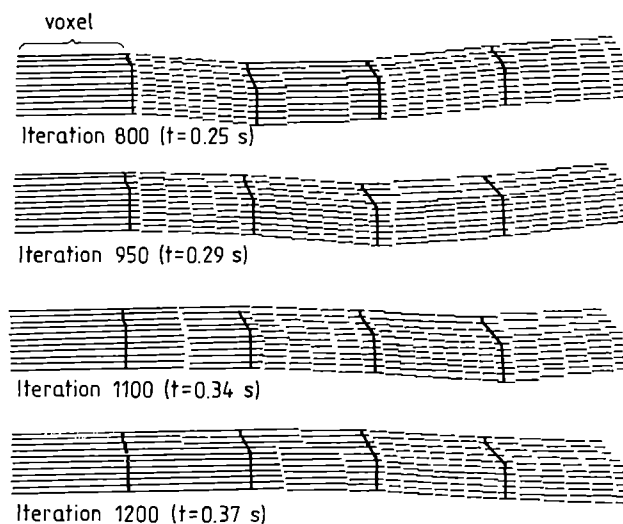


Fig. 10. Computer simulation of the polymer shrinkage at different times in the case of a parallelepipedic laser beam [5, 54]

The deformation can be strongly decreased by several ways [5]:

- employing as high-molecular as possible oligomeric components, consistent with maintaining a relatively low formulation viscosity (however, the high viscosity of the resin composite can act as a support);
- using monomers with very low shrinkage;
- the internal part of the object, should be polymerized, so that deformation will concern only a small volume of a polymer;
- using a pulsed rather than a continuous laser irradiation;
- controlling the intensity of the photon flux and irradiation time or the light displacement (dashed polymerization);
- adding porous fillers [66].

APPLICATIONS OF 3D-SL MODELS

3D-stereolithographic models (3D-SL) are readily scaled, quickly produced, and some 3D-SL models provide final parts with mechanical properties well suited for dynamic testing [71, 72]. Model testing has long been used to validate, augment, or replace structural analysis. Experimental modelling is performed for three basic reasons: to validate analysis, to augment analysis, or to replace analysis. Experimental models can have a number of characteristics that make them attractive, compared to testing actual components. Table 13 lists several of these features.

Table 13. Advantages of experimental methods [18]

Features	Examples
1. Enlarge small things	Turbine blades
2. Reduce small things	Wind tunnel aircraft and automotive models
3. Utilize special properties	Photoelastic testing of transparent model
4. Simplify testing	Fewer massive fixtures, smaller test loads
5. Results available earlier	Easily machined materials and now RP&M
6. Functional similarity	Fluid flow structure
7. Accelerate test development	Dress rehearsal for testing the real part
8. Geometric verification	Mock-ups

The latest new development in the 3D-SL technology is production of ceramic three dimensional parts using a ceramic slurry containing alumina powder and photoreactive resin [73—76].

End note: This article has been written by Dr. Julita Jakubiak, Head of an international joint project "Mechanisms, kinetics and applications of photopolymerization initiated by visible light photoinitiators", supervised by Prof. J. F. Rabek. Dr. J. Jakubiak spent one year (1998/1999) as post-doc researcher at the Polymer Research Group, Department of Dental Biomaterial Science, Karolinska Institute, The Royal Academy of Medicine, Stockholm, Sweden (directed by Prof. J. F. Rabek) and one year (1999/2000) as post-doc researcher at Laboratoire de Photochimie Generale, CNRS, University of Mulhouse, France (directed by Prof. J. P. Fouassier). The Authors gratefully acknowledge Prof. K. Yamaguchi of the Department of Mechanical Engineering, School of Engineering, Nagoya University, Japan, Prof. K. Skalski of the Institute of Mechanics and Design, Faculty of Production Engineering, Warsaw University of Technology, Poland, Prof. J. Pączkowski of the Department of Physical Chemistry, University of Technology and Agriculture, Bydgoszcz, Po-

land, and Ms. Mary Woods, Public Relations Mgr, 3D Systems, Valencia, CA, USA and European Office, 3D Systems, GmbH, Germany, for providing excellent materials, photographs and reference books enabling this review paper to be written.

REFERENCES

- [1] US Patent 2 755 758 (1956). [2] Herbert A. J.: *J. Appl. Photogr. Eng.* 1982, 8, 185. [3] Schwerzel R. E., Wood V. E., McGinness V. D., Weber C. M. *SPIE, Appl. Lasers Ind. Chem.* 1984, 90, 548. [4] US Patent 4 575 330 (1986). [5] Cabrera M., Jézéquel J. Y., André J. C. in: "Lasers in Polymer Science and Technology", Vol. III (ed. Fouassier J. P., Rabek J. F.), CRC Press, Boca Raton, Florida 1990, p. 73. [6] Wu D. S.: *Laser Focus World* 1990 (Nov.), 99. [7] Lindsay K. F.: *Modern Plastics* 1990 (Aug.), 40. [8] Neckers D. C.: *Chem. Tech.* 1990 (Oct.), 615. [9] Deitz D.: *Mech. Eng.* 1990 (Feb.), 34. [10] Peiffer R. W.: Proc. RadTech'91, Europe, Edinburgh 1991, p. 452. [11] Ashley S.: *Mech. Eng.* 1991 (April), 34. [12] Nakagawa T., Imamura M., Meng T., Wei J., Makinouchi A.: Proc. 3rd Intern. Conf. on Rapid Prototyping, University of Dayton, Dayton OH, USA 1992, p. 91. [13] Jacobs P. F.: "Rapid Prototyping & Manufacturing", Society of Manufacturing Engineers, MI, USA 1992. [14] Burns M.: "Automated Fabrication", PTR Prentice Hall, New Jersey, USA 1993. [15] Bernhard P., Hofmann M., Hunziker M., Klingert B., Schulthess A., Steinmann B.: in "Radiation Curing in Polymer Science and Technology" Vol. IV "Practical Aspects and Applications" (eds. Fouassier J. P., Rabek J. F.), Elsevier Applied Science, London 1993, p. 195. [16] Reynolds D. S.: in "Rapid Prototyping & Manufacturing Engineers, Deaborn 1992, p. 153. [17] André J. C., Corbel S.: "Stereophotolithographie Laser", Polytechnica, Paris, France 1994. [18] Jacobs P. F. (ed): "Stereolithography and Other RP&M Technologies: from Rapid Prototyping to Rapid Tooling", Society Manufacturing Engineers, Deaborn 1996. [19] Silicon Graphics Inc.: CAD/CAM/CAE Technology Review 1990. [20] Flach L., Chartoff R. P.: Proc. RadTech'90 North America, Chicago, Illinois, USA 1990, p. 52. [21] Flach L., Chartoff R. P.: "A Computer Model for Laser Photopolymerization in Solid Freeform Fabrication Proceedings" (ed. Beaman J. J.), University of Texas, Austin, Texas, USA 1990, p. 155. [22] Chartoff R. P., Flach L., Lightman A.: Proc. RadTech'91, Europe, Edinburgh 1991, p. 471. [23] Skalski K., Filipowski R., Świętoszkowski W., Kędzior K., Dąbrowski A.: *Mater. Proc. Techn.* 1998, 76, 49. [24] Watanabe T., Okawa M., Ukachi T.: Proc. RadTech'93 Asia, Tokyo, Japan 1993, p. 462. [25] Fouassier J. P.: "Photoinitiation, Photopolymerization, and Photocuring: Fundamentals and Applications", Hanser Publ., Munich 1995. [26] Rabek J. F.: "Mechanisms of Photophysical Processes and Photochemical Reactions in Polymers", Wiley, London 1987. [27] Decker

- C.: in "Radiation Curing in Polymer Science and Technology", Vol. III "Polymerization Mechanisms" (eds. Fouassier J. P., Rabek J. F.), Elsevier Applied Science, London 1993, p. 33. [28] Dietliker K. K.: "Chemistry & Technology of UV & EB Formulation for Coating, Inks & Paints" (ed. Oldring K. T.), Vol. 3., Sita Technology Ltd., London 1991, p. 239. [29] Neckers D. C., Jager W.: "Photoinitiation for Polymerization: UV & EB at the Millenium", Wiley, Chichester & Sita Technology Ltd., London 1998. [30] Fouassier J. P., Jacques P., Lougnot D. J., Pilot T.: *Polym. Photochem.* 1984, 5, 57.
- [31] Fouassier J. P.: *Progr. Org. Coat.* 1990, 18, 229. [32] Fouassier J. P., Ruhlmann D., Graff B., Morlet-Savary F., Wieder F.: *Progr. Org. Coat.* 1995, 25, 235. [33] Crivello J. V. in "UV Curing: Science and Technology", Vol. I (ed. Pappas S. P.), Technology Marketing Corp., Norwalk CT 1978, p. 23. [34] Green G. E., Stark P. P., Zahir S. A.: *J. Macromol. Sci. Rev. Macro. Chem.* 1981/1982, C21, 187. [35] Crivello J. V.: *Adv. Polym. Sci.* 1997, 62, 3. [36] Crivello J. V.: *J. Radiat. Curing.* 1997, 4, 2. [37] Crivello J. V., Lam J. H. V.: *J. Polym. Sci. Polym. Chem. Ed.* 1978, A16, 2441. [38] Rutsch W., Angerer H., Desorby V., Dietliker K., Hüsler R.: in Proc. 14th Intern. Conf. Org. Coat. Sci. Technol. Athens, 1990, p. 143. [39] Buhr G., Dammel R., Lindley C. R.: *Polym. Mater. Sci. Eng.* 1989, 61, 269. [40] Timpe H. J., Jockusch S., Körner K.: "Radiation Curing in Polymer Science and Technology", Vol. II Photoinitiating Systems" (eds. Fouassier J. P., Rabek J. F.), Elsevier Applied Science, London 1993, p. 575.
- [41] Neckers D. C., Hassoon S., Klimtchuk E.: *J. Photochem. Photobiol., A: Chem.*, 1996, 103, 95. [42] Lindén L.Å., Rabek J. F., Pączkowski J., Wrzyszczyński A.: *Polimery* 1999, 44, 161. [43] Eaton D. F.: *Adv. Photochem.* 1986, 13, 427. [44] Timpe H. J., Baumann H.: "Photopolymere; Prinzipien und Anwedungen", VEB Deutsche Verlag für Grundstoffindustrie, Leipzig 1985. [45] Fouassier J. P.: in "Processes in Photoreactive Polymers" (eds. Krongauz V. V., Trifunac A. D.), Chapman & Hall, New York 1995, p. 59. [46] Yamaoka T., Naitoh K.: in "Processes in Photoreactive Polymers" (eds. Krongauz V. V., Trifunac A. D.), Chapman & Hall, New York 1995, p. 111. [47] Jakubiak J., Rabek J. F.: *Polimery* 1999, 44, 447. [48] Tamura Y., Hagiwara T.: Proc. RadTech'97 Asia, Osaka, Japan 1997, p. 602. [49] Sitzmann E. V., Brautigam R. J., Srivastava C. M., Green G. D.: Proc. RadTech'92 North America, Northbrook, Illinois, USA 1992, p. 57. [50] Decker C.: in "Processes in Photoreactive Polymers" (eds. Krongauz V. V., Trifunac A. D.) Chapman & Hall, New York 1995, p. 34.
- [51] Jakubiak J., Rabek J. F.: *Polimery* 2000, 45, 485. [52] Duclos A. M., Jézéquel J. Y., Corbel S., André J. C.: *J. Photochem. Photobiol. A: Chem.* 1993, 70, 285. [53] Duclos A. M., Jézéquel J. Y., Corbel S., André J. C.: *J. Photochem. Photobiol. A: Chem.* 1994, 78, 85. [54] Takagi T., Nakajima N.: Proc. RadTech'93 Asia, Tokyo, Japan 1993, p. 451. [55] Schwerzel R. E., Wood E., Mc Grinniss V. D., Weber C. M.: *Appl. Lasers Ind. Chem.* 1984, 90, 548. [56] Yamaguchi K.: Proc. RadTech'97 Asia, Osaka, Japan 1997, p. 610. [57] Schwerzel R. E., Ivancič W. A., Johnson D. R., McGinnis V. D., Vood V. D., Jenkins V. E., Kramer J. A., Swainson W. K.: US Air Force Final Technical Report 1984. [58] McGimpsey W. G.: in "Lasers in Polymer Science and Technology" Vol. II (eds. Fouassier J. P., Rabek J. F.), CRC Press, Boca Raton, Florida 1990, p. 77. [59] Scaiano J. C., Johnston L. J., McGimpsey W. G., Weir D.: *Acc. Chem. Res.* 1988, 21, 22. [60] Brauschle C., Burland D. M.: *Angew. Chem. Intern. Ed.* 1983, 22, 582.
- [61] McGimpsey W. G., Scaiano J. C.: *Chem. Phys. Lett.* 1987, 13, 138. [62] McGimpsey W. G., Scaiano J. C.: *J. Am. Chem. Soc.* 1988, 110, 2299. [63] Braüchle C., Wild U. P., Burland D. M., Björklund G. C., Alvarez D. C.: *IBM Res. Dev.* 1982, 26, 1982. [64] Peiffer R. W.: Proc. RadTech'93 Asia, Tokyo, Japan 1993, p. 435. [65] Schaeffer P., Bertsch A., Corbel S., Jézéquel J. Y., André J. C.: *J. Photochem. Photobiol. A: Chem.* 1997, 107, 283. [66] Karrer P., Corbel S., André J. C., Lougnot D. J.: *J. Polym. Sci., Polym. Chem. Ed.* 1992, 30, 2715. [67] Chikaoka S., Ohkawa K.: Proc. RadTech'93 Asia, Tokyo, Japan 1993, p. 468. [68] Marutani Y., Nakai T.: *Laser Research* 1989, 17, 410. [69] Hunziker M.: in "Rapid Prototyping & Manufacturing" (ed. Jacobs P. F.), Society Manufacturing Engineers, Dearborn 1992, p. 25. [70] Krajewski J. J.: *J. Coat. Technol.* 1990, 62, 73.
- [71] Dornfeld W.: in "Stereolithography and Other RP&M Technologies: from Rapid Prototyping to Rapid Tooling" (ed. Jacobs P. F.), Society Manufacturing Engineers, Dearborn 1996, p. 329. [72] Jacobs P. F.: in "Stereolithography and Other RP&M Technologies: from Rapid Prototyping to Rapid Tooling" (ed. Jacobs P. F.), Society Manufacturing Engineers, Dearborn 1996, p. 318. [73] Griffith M. L., Halloran J. W.: *Manufacturing Sci. Eng.* 1994, 2, 529. [74] Griffith M. L., Halloran J. W.: *J. Am. Ceram. Soc.* 1996, 79, 2601. [75] Hinczewski C., Corbel S., Chartier T.: *J. Eur. Ceram. Soc.* 1998, 18, 583. [76] Hinczewski C., Corbel S., Chartier T.: *Rapid Prototyp. J.* 1998, 4, 104.